Information Theoretic Limits for Free-Space Optical Channels With and Without Memory

Stojan Z. Denic, *Member, IEEE*, Ivan Djordjevic, *Member, IEEE*, Jaime Anguita, *Member, IEEE, Member, OSA*, Bane Vasic, *Senior Member, IEEE*, and Mark A. Neifeld, *Member, IEEE, Fellow, OSA*

***Abstract*—The availability of Channel State Information (CSI) and the effects of channel memory on the capacities and the achievable rates of free-space optical communication channels are investigated. For memoryless channels, the capacities and achievable rates are computed and compared for both uniform and "positive" Gaussian inputs subject to different assumptions on the CSI availability. For the strong turbulence regime, it is shown that the knowledge of CSI both at the transmitter and the receiver increases the achievable rates for low-to-moderate Signal-to-Noise Ratios (SNRs) in comparison to the cases for which the CSI is known only at the receiver. For the weak turbulence regime however, the availability of CSI at both ends of the link does not provide any improvement over a system with CSI known at the receiver alone, and we find that a simple channel inversion technique suffices. In addition, for low SNRs, Pulse Amplitude Modulation (PAM) with $M \geq 4$ levels outperforms Gaussian-distributed inputs regardless of the knowledge of CSI at the transmitter. For high SNRs, a Gaussian distribution gives superior results, implying the need for new, more efficient positive signal constellations. For channels with memory and without knowledge of CSI, a change in the channel quasifrequency has negligible effects on the capacity for any turbulence regime.**

***Index Terms*—Achievable rate, capacity, channels with memory, fading channels, free-space optical communications.**

I. Introduction

THE performance of any communication system can be significantly affected by the channel memory and the availability of the channel state information (CSI) [1]. The goal of this paper is to study the capacities and achievable rates for free-space optical (FSO) communication channels subject to different assumptions on the channel memory and the knowledge of CSI. It extends the work done in [2].

The focus is on intensity modulation/direct detection (IM/DD) FSO systems subject to different degrees of optical turbulence (inducing intensity fluctuation on the received signal) and additive white Gaussian noise (AWGN) introduced by the receiver electronics. To cover both the strong and the weak turbulence regimes, the received signal intensity fluctuations are modeled by a gamma-gamma distribution [3].

With respect to the channel memory assumption, two scenarios are investigated: 1) intensity fluctuations are temporally independent and identically distributed (IID) and 2) intensity fluctuations are described by a Markov model. It should be noted that the results for an IID model can be applied to the so-called block-fading channels under the assumption that the channel fluctuations correspond to a stationary and ergodic random process [4].

For the IID scenario, two input distributions are considered: 1) discrete uniform and 2) "positive" Gaussian (i.e., a Gaussian distribution that generates inputs which are positive with probability close to 1). Such input distributions are chosen for two reasons. First, an input distribution that maximizes the mutual information under the average optical power constraint for the positive input is not known in general [5]. Secondly, a "positive" Gaussian input (for which the mutual information can be computed [6]) will help us gain intuition on the behavior of the achievable rates under different CSI assumptions. A Gaussian input distribution for FSO channels is investigated in [7]. As we will show, for the strong turbulence regime and low-to-moderate SNRs, the knowledge of CSI at both the transmitter and the receiver gives a higher achievable rate than that of the case for which the CSI is present at the receiver only. This means that adaptive communication strategies (i.e., those using feedback and adaptive coding), can be beneficial. For weak turbulence regimes, knowing the CSI at the transmitter is no longer beneficial. In this case a simple technique of channel inversion is possible, enabling the use of codes for AWGN channels. In both regimes, for low SNRs, the "positive" Gaussian inputs yields lower achievable rates than $M \geq 4$ PAM. However, for high SNRs, the Gaussian input distribution is more efficient than the PAM. Thus, it follows that larger multilevel (than the currently used $M = 2$) and more efficient signal constellations have to be designed to approach the channel capacity upper bound found in [8].

In the case of FSO channels with memory, a Markov model is used (which is a generalization of the Gilbert-Elliot model [9], [10]) that assumes no knowledge of CSI at either the transmitter or the receiver. To extract a transmitted signal, the receiver uses the knowledge of the communication channel distribution, which is commonly referred to as channel distribution information (CDI). The channel capacity is computed for strong and weak turbulence regimes and for different values of the

Manuscript received November 9, 2007; revised March 25, 2008. Current version published December 19, 2008. This work was supported in part by the NSF under Grants CCF-0634969, ITR-0325979, and IHCS-0725405.

S. Z. Denic was with the Department of Electrical and Computer Engineering, University of Arizona, Tucson, AZ 85721 USA. He is now with Toshiba Telecommunications Research Laboratory, Bristol BS1 4ND, U.K. (e-mail: Stojan.Denic@toshiba-trel.com).

I. Djordjevic, J. Anguita, B. Vasic, and M. A. Neifeld are with the Department of Electrical and Computer Engineering, University of Arizona, Tucson, AZ 85721 USA (e-mail: ivan@ece.arizona.edu; janguita@ece.arizona.edu; vasic@ece.arizona.edu; mark@ece.arizona.edu).

Color versions of one or more of the figures in this paper are available online at http://ieeexplore.ieee.org.

Digital Object Identifier 10.1109/JLT.2008.925669

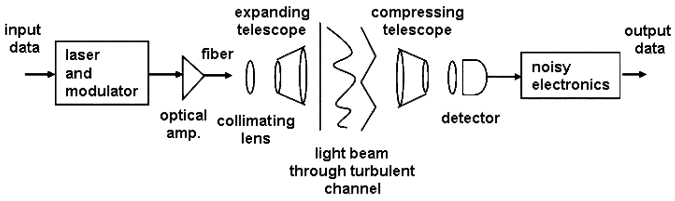

Fig. 1. Block diagram of a typical FSO communication system.

channel quasifrequency. Quasifrequency is a parameter analogous to Doppler spread found in radio-frequency (RF) fading channels, and it represents a measure of the effective bandwidth of the turbulence-induced signal fluctuations [11]. From extensive measurements, it is determined that a practical range for the quasifrequency is between 100 Hz and 500 Hz. Numerical results also show little change in the capacity as a function of quasifrequency.

The capacity computations in the paper are carried out for a simple modulation format such as PAM. Because FSO channel is envisioned as the solution to the connectivity bottleneck problem and as a supplement to wireless links, the complexity of transmitter and receiver must be low. Therefore, IM/DD is proposed as a reasonable choice for FSO links. Since the negative signal cannot be transmitted over an FSO link with direct detection, PAM is a viable modulation format. Other multilevel schemes, such as those based on quadrature amplitude-modulation require the use of dc bias, and the power efficiency of such schemes is low.

Previous work on the FSO channel capacity in the presence of AWGN includes [5], [8], and [12]. The analysis of the FSO communication system performance in terms of the bit error rate may be found in [13], [14]. Some practical communication schemes are discussed in [15].

The paper is organized as follows. In Section II, the FSO communication system and the channel model are described. In Section III, the capacities and achievable rates are provided for IID FSO channels. Section IV gives the capacity of FSO channels with memory based on the Markov channel model.

II. FSO Communication System

A typical FSO communication system, shown in Fig. 1, consists of a transmitter, propagation path through the atmosphere, and receiver. The optical transmitter includes a light source (i.e., a semiconductor laser of high launch power and wide bandwidth) and a telescope assembly designed using either lenses or a parabolic mirror. A data stream carrying information modulates the light source. The modulated beam is projected toward the receiver. Along the propagation path through the atmosphere, the light beam is subject to absorption, scattering and optical turbulence, which cause light attenuation, random variations in the light wave amplitude and phase, and beam wandering. At the receiver, an optical system collects the light and focuses it onto a detector, which delivers an electrical current proportional to the power of the incoming light. If error correction codes are used, the input electrical data stream is encoded before transmission and later decoded at the receiver after the optical-to-electrical conversion.

An FSO communication channel is described by

$$y_t = i_t x_t + n_t \tag{1}$$

where $x \triangleq \{x_t\}_{t\geq 0}$ is the transmitted signal, $i \triangleq \{i_t\}_{t\geq 0}$ is the instantaneous intensity gain, $n \triangleq \{n_t\}_{t\geq 0}$ is the AWGN having a normal distribution $N(0,\sigma^2)$, and $y \triangleq \{y_t\}_{t\geq 0}$ is the received signal. All above signals are real-valued. In the performance analysis, different types of constraints on the transmitted signal x are assumed, such as peak and average-power constraint. The transmitted signal x may be positive or zero, since we deal with IM systems. The Gaussian noise models the thermal noise of the receiver electronics. It is assumed that i is stationary and ergodic and that the effective photo-current conversion ratio of the receiver is included in i.

In all numerical examples, the achievable rate curves are plotted versus average SNR at the receiver, defined by $SNR \triangleq PE\left[i_t^2\right]/\sigma^2$, where $E\left[x_t^2\right] \leq P$. Although it has been already employed in [12] for studying the performance of FSO communication systems, this definition is somewhat different than the one usually used in FSO communications, which is given by either $E^2[i_t]/N_0$ or P_o/σ, where $N_0/2 = \sigma^2$, and $E[x_t] \leq P_o$[8]. The definition used here is common for RF fading channels and emphasizes the role of the receiver, whose performance depends on the average power of the electrical current, obtained by the conversion from the optical signal. In the case of FSO systems, this average power is given by $PE\left[i_t^2\right]$. Moreover, for all input distributions used in this paper, there exists a correspondence between the average power of the optical signal $E[x_t]$ and the average power of the electrical current at the receiver such that a system performance can be presented by using one or the other definition of the SNR. And finally, the achievable rate obtained by using the $E\left[x_t^2\right] \leq P$ constraint is a lower bound on the achievable rate obtained by using $E[x_t] \leq P$ constraint since the set of input signals defined by the former constraint is the subset of the set of input signals defined by the latter.

A. Intensity Fluctuation Model

The intensity fluctuation of the received signal in the FSO system is caused by the so-called optical turbulence. The most widely used model for the optical turbulence is due to Kolmogorov [11]. His model envisions a number of floating cells (eddies) of different sizes containing cool air, which are surrounded by warm air. Each eddy acts like a random focusing lens (having random index of refraction) on the propagating optical wave, causing intensity fluctuations (fading) of the received signal. Associated with the size of eddies, two parameters are defined: 1) L_0, the effective outer scale of turbulence and 2) l_0, the effective inner scale of turbulence [11]. These two parameters are of interest because they are used to define different regimes of optical turbulence.

Another parameter of interest, which is used to describe the fluctuation of the intensity of the optical wave is called the scintillation index, and is defined by

$$\sigma_I^2 \triangleq \frac{E\left[i_t^2\right]}{E^2[i_t]} - 1. \tag{2}$$

Weak turbulence regimes are those for which the scintillation index is less than one. The scintillation index is proportional to the so-called Rytov variance defined by

$$\sigma_R^2 = 1.23 C_n^2 k^{7/6} L^{11/6}$$

where $k = 2\pi/\lambda$ is the wavenumber, λ is the optical wavelength, L is the propagation distance, and C_n^2 is the refractive index structure parameter [11]. C_n^2 is assumed to be constant for horizontal propagation paths [11]. Rytov variance is commonly used in weak turbulence regimes, but it can also be employed as a measure for strong turbulence, by increasing C_n^2 or L. For strong turbulence regimes, the scintillation index is greater than or equal to one. To characterize the strength of the turbulence, both scintillation index and Rytov variance are used in this paper.

To determine the reliability of a communication link, an accurate probabilistic model for the intensity fluctuations is necessary. Based on the measurements and propagation model analysis, several probability density functions (PDFs) have been proposed for the instantaneous intensity gain i[11]. Here, we adopt a gamma-gamma PDF proposed by Al-Habash *et al.* [3], because it can be applied to model both weak and strong turbulence regimes. It is given by

$$p(i_t) = \frac{2(\alpha\beta)^{(\alpha+\beta)/2}}{\Gamma(\alpha)\Gamma(\beta)} i_t^{(\alpha+\beta)/2-1} K_{\alpha-\beta}(2\sqrt{\alpha\beta i_t}) \quad (3)$$

where $i_t > 0$, α, and β are parameters of the PDF, $\Gamma(\cdot)$ is the gamma function, and $K_{\alpha-\beta}(\cdot)$ is the modified Bessel function of the second kind of order $\alpha-\beta$. The mean value of a gamma-gamma PDF is $E[i_t] = 1$, while the second moment is given by $E\left[i_t^2\right] = (1+1/\alpha)(1+1/\beta)$. The parameters α and β and the scintillation index σ_I^2 are related through $\sigma_I^2 = 1/\alpha + 1/\beta + 1/\alpha\beta$[3].

Another important parameter in the analysis of turbulence is the expected number of fades per unit time $E[n(i_T)]$[11]. It is related to the number of crossings of a prescribed turbulence threshold. It will be used to determine the transition probabilities of the Markov fading model [10]. The formula for the expected number of fades was derived by Rice, and for a gamma-gamma distribution is given by

$$\frac{2\sqrt{2\pi\alpha\beta}\nu_0\sigma_I}{\Gamma(\alpha)\Gamma(\beta)} \left(\frac{\alpha\beta i_T}{E[i_t]}\right)^{(\alpha+\beta)/2-1} K_{\alpha-\beta}\left(2\sqrt{\frac{\alpha\beta i_T}{E[i_t]}}\right) \quad (4)$$

where i_T is a prescribed threshold, and ν_0 is the quasifrequency which determines the channel memory.

III. Achievable Rates for IID FSO Channels With CSI

In this section, the achievable rate and capacity formulas are provided for two input distributions, discrete uniform and "positive" Gaussian, and for four different assumptions regarding the availability and usage of the CSI at the transmitter and the receiver. Although it is supposed that i is an IID process, since it is stationary and ergodic, the results are also applicable to slowly varying (block-fading) channels, when the message is long enough to reveal long-term ergodic properties of the turbulence process [4].

A. Achievable Rates for "Positive" Gaussian Distribution

Next, we consider achievable rates for the "positive" Gaussian input. A "positive" Gaussian input refers to a Gaussian input signal x having a positive mean A. The "positive" Gaussian input is employed in order to provide the positivity of almost all values of the transmitted signal x. In simulations, we add a bias A equal to $4\sigma_x$ or $5\sigma_x$, where σ_x^2 represents the variance of the transmitted signal x. This means that 99.99% of the transmitted signal values are within interval of $\pm 4\sigma_x$ or 99.9999% for $\pm 5\sigma_x$. However, the price has to be paid in terms of the power efficiency, since the bias A conveys no information. Here, $E[x_t] = A = c\sigma_x$, $c \in \{4, 5\}$, implying $E\left[x_t^2\right] = \sigma_x^2 + A^2 = (1+c^2)\sigma_x^2$, giving direct connection between two definitions of the SNR discussed in Section II.

1) *Complete CSI at the transmitter and the receiver*. In this case, both the transmitter and the receiver have complete knowledge regarding the realization of i. This corresponds to the situation when the receiver estimates the channel, and sends this information to the transmitter by using perfect feedback. This is plausible scenario for FSO channels, since the turbulence changes slowly relative to the large symbol rate. Because the CSI is available at the transmitter, the transmitter is able to maximize the mutual information subject to power constraint by adapting a power control policy to the value of i. If $P(i_t)$ denotes a power policy, then the achievable rate is given by

$$R_{tr} = \int_{\mathcal{I}} B \log\left(\frac{i_t^2 P\mu}{\sigma^2}\right) p(i_t) di_t \quad (5)$$

$$\int_{\mathcal{I}} P(i_t) p(i_t) di_t = \int_{\mathcal{I}} \left(\mu - \frac{\sigma^2}{i_t^2 P}\right) p(i_t) di_t = 1 \quad (6)$$

where $\mathcal{I} \triangleq \left\{i_t : \mu - \sigma^2/i_t^2 P > 0\right\}$, $\mu > 0$, and B is the bandwidth of the transmitted signal x. This is a standard formula for the channel capacity, and (6) is a water-filling equation [6].

2) *Complete CSI at the receiver*. In this case, only the receiver has complete knowledge regarding the realization of process i. The achievable rate is given by

$$R_r = \int_{\mathbf{R}^+} B \log\left(1 + \frac{i_t^2 P}{\sigma^2}\right) p(i_t) di_t \quad (7)$$

where $\mathbf{R}^+$ is the set of positive real numbers. This corresponds to an FSO system which does not use a feedback.

3) *Channel inversion.* Channel inversion represents a simple communication technique, where the transmitter adapts its power policy to keep a constant level of the SNR, $\Gamma(i_t) \triangleq i_t^2 P(i_t)/\sigma^2$, at the receiver side. The power adaptation policy is defined by $P(i_t) = K/i_t^2$, so that the SNR is given by $\Gamma(i_t) = K/\sigma^2$, and $K = P/E\left[1/i_t^2\right]$. Upon the channel inversion, we deal with a standard AWGN

channel with SNR, $P/\sigma^2 E\left[1/i_t^2\right]$. The achievable rate for the channel inversion is given by

$$R_{inv} = B\log\left(1+\frac{P}{\sigma^2 E\left[\frac{1}{i_t^2}\right]}\right). \tag{8}$$

Similar to the analysis in [6] for Rayleigh fading, for FSO channels, the usefulness of channel inversion depends on the values of the parameters α and β of the gamma-gamma distribution that determine the value of $E\left[1/i_t^2\right]$. If $(\alpha+\beta)/2-1$ is large enough (see (3)) such that $i^{(\alpha+\beta)/2-1}$ dominates i_t^2, $E\left[1/i_t^2\right]$ will not be very large number for small values of i_t (consequently the capacity will be positive), and the channel inversion could be useful simple communication technique for FSO systems. In the opposite case, $E\left[1/i_t^2\right]$ is large, and the achievable rate tends zero.

4) *Truncated channel inversion.* As it was pointed out, the problem with the channel inversion is that this technique may be detrimental for certain values of the parameters α and β. This is why, a truncated inversion is proposed in [6]. The basic idea underlying truncation is to apply the channel inversion only when the irradiance i is above some threshold $i_0>0$, to prevent $E\left[1/i_t^2\right]$ going infinity. Thus

$$P(i_t) = \begin{cases} \frac{K}{i_t^2} & i_t \geq i_0 \\ 0 & i_t < i_0. \end{cases} \tag{9}$$

Then, the achievable rate for this case is given by

$$R_{tinv} = \max_{i_0>0}\left\{B\log\left(1+\frac{P}{\sigma^2 E_{i_0}\left[\frac{1}{i_t^2}\right]}\right)\Pr\{i_t\geq i_0\}\right\} \tag{10}$$

where $E_{i_0}\left[1/i_t^2\right] \triangleq \int_{i_t\geq i_0} 1/i_t^2 p(i_t)di_t$, and $\Pr\{i_t \geq i_0\} \triangleq \int_{i_t\geq i_0} p(i_t)di_t$.

B. Achievable Rates for PAM Signaling and Uniform Input Distribution

For this study, we assume the transmitted signal x takes values from the set $\chi \triangleq \{0, d, \ldots, d(M-1)\}$, $M\geq 2$, where d defines the distance between two points in the signaling set. If all the signal levels are assumed to be equiprobable, the average energy is given by $E\left[x_t^2\right] = d^2(M-1)(2M-1)/6$. Since $E[x_t] = d(M-1)/2$, a direct relation between the two SNR definitions can be established as in the Gaussian case. The conditional distribution of the received signal is given by

$$p(y_t|i_t) = \frac{1}{M}\sum_{x_t\in\chi} p(y_t|x_t, i_t) \tag{11}$$

where

$$p(y_t|x_t,i_t) = \frac{1}{\sqrt{2\pi}\sigma}e^{-(y_t-i_t x_t)^2/2\sigma^2}. \tag{12}$$

When the CSI is present at the receiver, but not at the transmitter, the achievable rate for this input signal is given by the conditional mutual information between the transmitted signal x and the received signal y, conditioned on the CSI i[1]

$$\begin{aligned} I(x_t;y_t|i_t) &= E[h(y_t|i_t) - h(n_t|i_t)] \\ &= E\left[-\frac{1}{M}\sum_{x_t\in\chi}\int_{\mathbf{R}} p(y_t|x_t,i_t)\log p(y_t|i_t)dy_t\right] \\ &\quad -\frac{1}{2}\log(2\pi e\sigma^2) \end{aligned} \tag{13}$$

where E denotes the expectation with respect to the distribution $p(i_t)$, $h(\cdot)$ is the differential entropy, and $\mathbf{R}$ is the set of real numbers. For $M=2$, (13) represents the Shannon capacity when the CSI is available at both the transmitter and the receiver or at the receiver only. The first claim comes from the symmetry of the channel for $M=2$, while the second is the consequence of the compatibility conditions [6].

To clarify the first statement, observe that when the CSI is present at the transmitter and the receiver, the communication channel is equivalent to the AWGN channel with binary input and continuous output. Then, the mutual information for each particular realization of the channel i is maximized by $\Pr\{x_t = 0\} = \Pr\{x_t = d\} = 1/2$, which is given by the argument of the expectation $E[\cdot]$ in (13). Since the channel i varies according to distribution $p(i_t)$, the channel capacity is given by the expectation over $p(i_t)$[6].

The compatibility conditions are satisfied if 1) the channel input is IID and 2) the mutual-information-maximizing input distribution $\Pr\{x=x_0\}$, $x_0\in\chi$, is the same regardless of the CSI i. Then

$$\max_{\Pr\{x_t=x_0\}} E[I(x_t;y_t|i_t)] \tag{14}$$

$$E[\max_{\Pr\{x_t=x_0|i=i_0\}} I(x_t;y_t|i_t=i_0)]. \tag{15}$$

The left-hand side is the channel capacity when the CSI is present at the receiver only, while the right-hand side corresponds to the channel capacity when both the transmitter and the receiver have the CSI.

The numerical results and analysis of the achievable rates for uniform PAM inputs are presented in Section III-C.

C. Examples

Fig. 2 shows the achievable rates for uniform PAM signaling when $M=2, 4, 8$, and 16, and for the "positive" Gaussian input, $A=4\sigma_x$, when four different transmitter/receiver strategies are applied. Here, the values of the parameters are $\alpha=10$, $\beta=1$, which corresponds to the strong turbulence regime with $\sigma_R=6$, $\sigma_I^2=1.2$, and $l_0=0$. In addition, Fig. 2 shows the upper bound on the capacity C_{ub}, found in [8], averaged over the gamma-gamma distribution.

In the case of the positive Gaussian input, the computations show that CSI at the transmitter side may contribute to the increase in the achievable rate by 60% at 10 dB ($R_r=0.22$ bits/channel use versus $R_{tr}=0.35$ bits/channel use), 30% at 16 dB ($R_r=0.5$ bits/channel use versus $R_{tr}=0.65$ bits/channel use), and 17% at 20 dB ($R_r=0.8$ bits/channel use versus $R_{tr}=0.93$ bits/channel

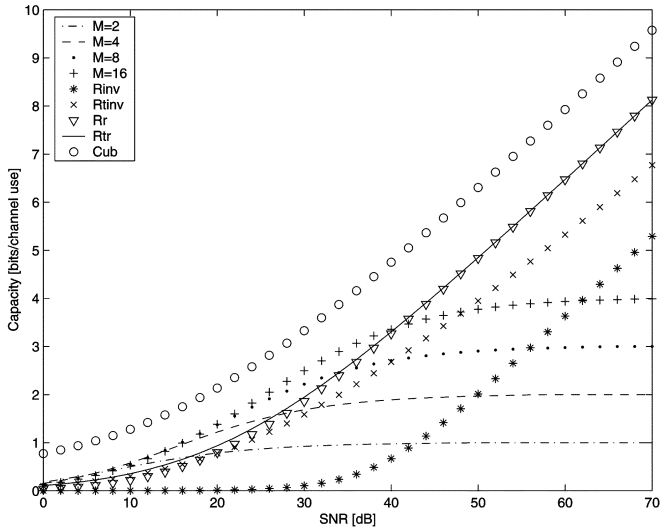

Fig. 2. Achievable rate versus SNR for strong turbulence for "positive" Gaussian $A = 4\sigma_x$.

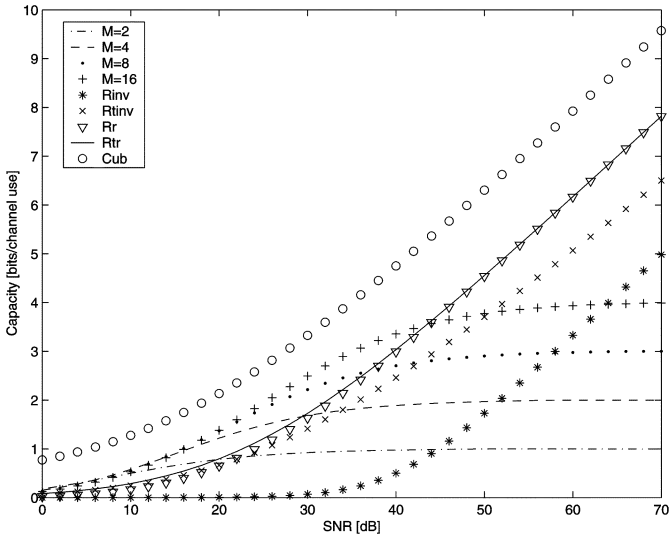

Fig. 3. Achievable rate versus SNR for strong turbulence for "positive" Gaussian $A = 5\sigma_x$.

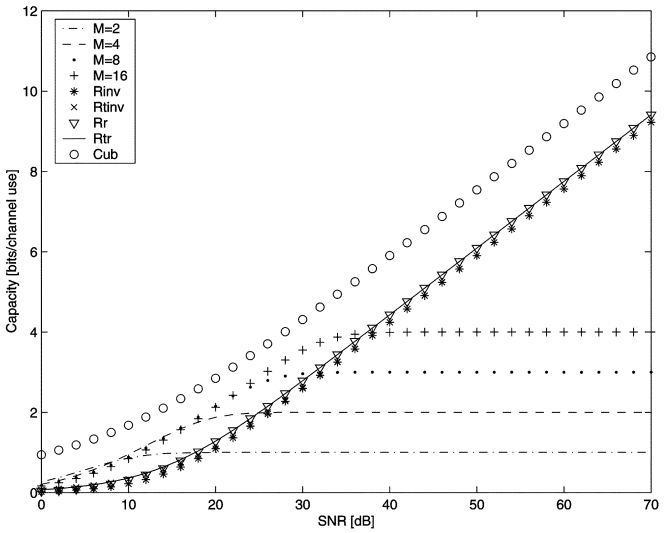

Fig. 4. Achievable rate versus SNR for weak turbulence for "positive" Gaussian $A = 4\sigma_x$.

use). This points out the difference between FSO fading and RF fading, where the contribution to the capacity of the CSI at the transmitter is negligible. A reason for this might be more detrimental nature of FSO fading comparing to the RF fading. This would mean that in the case of FSO fading, the CSI at the receiver only is not enough to achieve the maximum of the mutual information; in addition, the CSI at the receiver has to be utilized.

For higher SNRs there is no benefit of the CSI at the transmitter relative to the case of the CSI at the receiver only. Thus, the feedback in FSO systems can bring benefit at low to moderate SNRs. In the case of the channel inversion, the achievable rate is zero for reasonably high SNRs, as in the case of the Rayleigh RF fading (Nakagami fading with $m = 1$). The truncated channel inversion shows weaker performance than the case when the CSI is available at the transmitter and the receiver.

Comparing to the uniform PAM signaling, we notice that the "positive" Gaussian distribution can have worse performance below some threshold SNR. For instance, for $M = 2$, this threshold is at 17 dB, and for $M = 4$, the threshold is at 27 dB. Thus, On-Off Keying (OOK) is not optimal signaling for moderate and high SNRs. To improve capacity, one should consider PAM systems with $M = 4$, $M = 8$ or $M = 16$. Fig. 2 shows that the PAM with $M = 16$ is 7 dB away from the upper capacity bound at 25 dB, while the positive Gaussian exhibits a constant distance of 9 dB from the capacity bound. To improve the capacity, we obviously need to design new signal constellations that will take into account a positivity condition.

Fig. 3 presents the achievable rates for strong turbulence when the bias is $A = 5\sigma_x$, for the same parameters as in Fig. 2. Although the bias is larger, the conclusions regarding the usefulness of the CSI remain unchanged. The only difference is that the larger bias causes the "positive" Gaussian input to suffer an additional loss of approximately 2 dB.

In Fig. 4, the achievable rates are presented for $\alpha = 17.13$, $\beta = 16.04$, corresponding to a weak turbulence regime with $\sigma_R = 0.01$, $\sigma_I^2 = 0.124$ taken from [3]. Here, the bias is again $A = 4\sigma_x$. In the case of the "positive" Gaussian input, it can be noticed that the CSI at the transmitter does not give any advantage as compared to other strategies. Hence, one can use the channel inversion or the truncated channel inversion policy and employ codes for Gaussian channels. This means that a weak turbulence situation for FSO channels roughly corresponds to the Nakagami fading with a parameter $m > 1$ of the RF fading channel [6]. On the other hand, the PAM signaling is now even more effective than the Gaussian input for lower SNRs, and the PAM signaling with $M = 16$ is 4 dB away from the upper capacity bound at around 25 dB. Comparing with the strong turbulence channels, the weak turbulence channel capacity is noticeably larger. For instance, in the weak turbulence case and for $M = 2$, a required SNR to achieve the capacity of 1 bits/channel use is 32 dB, while in the strong turbulence case, 70 dB is required.

IV. Capacity of Markov FSO Channels

There are two qualitative differences between previously considered FSO channel models and the one studied in this section. First, a current channel model have memory, and secondly, channel information that is available is the CDI at the receiver, i.e., the receiver has the knowledge about the intensity gain distribution only, without any CSI present at the transmitter and/or receiver. Here, $M = 2$ PAM case is studied since it is anticipated that the computations for $M > 2$ would lead to similar conclusions.

A. Markov Channel Model

To model an FSO channel with memory, a generalized Gilbert-Elliot model is employed. This model was earlier used for modeling RF fading channels [10]. The idea is to divide the set of all possible values of the intensity gain $\mathbf{R}^+$ (real positive numbers) into a finite number of intervals $[I_k, I_{k+1})$, $k = 0, \ldots, K-1$, and to assign each interval to one state of a Markov chain $s \triangleq \{s_t\}_{t\geq 0}$, $s_t \in \{\sigma_0, \ldots, \sigma_{K-1}\}$. The transition probability of the Markov chain from k^{th} to j^{th} state is denoted by $p_{k,j}$, $0 \leq k, j \leq K-1$. Here, the same Markov model is employed as in [10], i.e., it is assumed that the transitions are possible only to neighboring states and to the current state. This is equivalent to fixing $p_{k,j} = 0$ for $|k-j| > 1$. To completely define the proposed model, the following issues have to be addressed: 1) how to compute the transition probabilities $p_{k,j}$, $0 \leq k, j \leq K-1$ and 2) how to determine the appropriate number of states K of the Markov chain model?

To determine transition probabilities, the notion of expected number of fades per unit time $E[n(i_T)]$ is employed [see (4)] [10]. $E[n(i_T)]$ can also be understood as the average number of crossings of level i_T[11]. Thus, the larger $E[n(i_T)]$ the less amount of time the channel spends at the specified intensity gain level i_T. If an interval of intensity gain levels is represented by the state σ_k of the Markov chain, then larger $E[n(I_k)]$ corresponds to larger transition probability $p_{k,k-1}$ to neighboring state σ_{k-1} and smaller $p_{k,k}$. This implies that the memory of the model tends to be smaller. This is the intuition behind the derivation of the formulas for the transition probabilities of the Markov chain FSO channel model which are given in [10]. An underlying assumption is that the FSO channel is slow-fading, i.e., the channel remains in the same Markov chain state during the duration of at least one channel symbol. Then, the transition probability formulas are determined in the following way. Suppose that the transmission rate is given by R symbols per second. Then, the average number of symbols per second transmitted in the k^{th} state is given by $R_k = p_{\sigma_k} R$. Since it is assumed that the channel is slow fading, the transition probabilities $p_{k,j}$, $0 \leq k, j \leq K-1$ can be approximated by [10]

$$p_{k,k+1} \approx \frac{E[n(I_{k+1})]}{R_k}, \quad k = 0, \ldots, K-2 \tag{16}$$

$$p_{k,k-1} \approx \frac{E[n(I_k)]}{R_k}, \quad k = 1, \ldots, K-1 \tag{17}$$

$$p_{k,k} = 1 - p_{k,k-1} - p_{k,k+1}, \quad k = 1, \ldots, K-2 \tag{18}$$

$$p_{0,0} = 1 - p_{0,1}, \quad p_{K-1,K-1} = 1 - p_{K-1,K-2}. \tag{19}$$

Remark IV.1: A parameter that determines the expected number of fades per unit time $E[n(i_T)]$ is the quasifrequency ν_0 which has been defined and computed by Rice in [16]

$$\nu_0 = \frac{1}{2\pi}\sqrt{-\frac{\psi''(0)}{\psi(0)}}, \tag{20}$$

where $\psi(\tau)$ is the autocorrelation function of the intensity gain process, and $\psi''(\tau)$ is its second derivative. As discussed in [11], also ν_0 roughly represents the standard deviation of the normalized Power Spectral Density (PSD) $\Psi(\omega)$, which corresponds to $\psi(\tau)$, when $\Psi(\omega)$ is understood as the probability density function. Therefore, it is possible to obtain the quasifrequency ν_0 from measurements, by first computing the autocorrelation function $\psi(\tau)$ and then applying the Rice formula (20).

The choice of appropriate number of states of the Markov model is another important issue. The number of states in fact affects the resolution or the accuracy of the model. Larger number of states means better model accuracy which in tern should give more precise estimate of the channel capacity. This question will be treated in more detail when a specific example of the channel is considered in Section IV-C.

Further, each state of the Markov chain is associated with a corresponding binary symmetric channel, having crossover probability $p_{e,k}, 0 \leq k \leq K-1$, which is in accordance with the OOK modulation at the transmitter. Here, the transmitted signal x takes values from the set $\{0, A\}$. To compute the crossover probability for each state, an error probability formula for OOK in the presence of a Gaussian noise is applied, which is given by $\Phi\left(\sqrt{\Gamma(i_t)/2}\right)$, where $\Phi(x) \triangleq 1/\sqrt{2\pi}\int_x^{+\infty} e^{-t^2/2}dt$, and $\Gamma(i_t) \triangleq i_t^2 E\left[x_t^2\right]/\sigma^2 = i_t^2 A^2/2\sigma^2$ is the SNR for a given value of i_t. Then, the crossover probability for the state σ_k is calculated by

$$p_{e,k} = \frac{\int_{I_k}^{I_{k+1}} \Phi\left(\sqrt{\frac{i_t^2 A^2}{4\sigma^2}}\right) p(i_t) di_t}{\int_{I_k}^{I_{k+1}} p(i_t) di_t}, \quad k = 0, \ldots, K-1. \tag{21}$$

Thus, the channel is restricted to the channel having discrete inputs and discrete outputs.

B. Capacity Formula

Assume that the transmitted and received signals are binary, $x_t, y_t \in \{0, 1\}$. Then, the Gilbert-Elliot model defines the error at the receiver as $z_t \triangleq x_t \oplus y_t$, where "$\oplus$" represents modulo-2 summation. Hence, a sequence $z \triangleq \{z_t\}_{t\geq 0}$ represents an error signal. Further, introduce the following notation for conditional probabilities:

$$q_k^*\left(z_0^{k-1}, s_0\right) \triangleq \Pr\left\{z_k = 1 | z_0^{k-1}, s_0\right\} \tag{22}$$

$$q_k\left(z_0^{k-1}\right) \triangleq \Pr\left\{z_k = 1 | z_0^{k-1}\right\} \tag{23}$$

where $z_0^{k-1} \triangleq (z_0, \ldots, z_k)$. It is proven in [9] that the channel capacity is given in terms of limits as follows:

$$C = 1 - \lim_{k\to+\infty} E[h(q_k)] \tag{24}$$

$$= 1 - \lim_{k\to+\infty} E\left[h(q_k^*)\right] \tag{25}$$

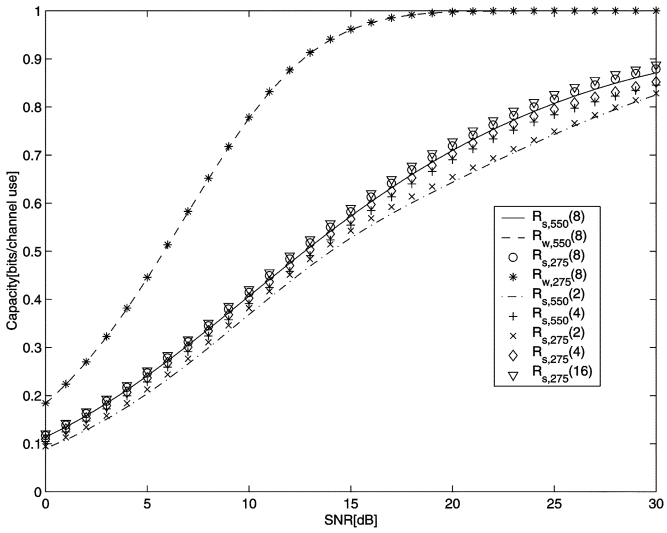

Fig. 5. Capacity versus SNR using OOK with quasifrequency as a parameter.

where $h(q) \triangleq -q\log_2 q - (1-q)\log_2(1-q)$. Here, (24) approaches the capacity from below, while (25) approaches it from above. The recursive expressions for computing (22) and (23) may be inferred from [9].

C. Example

Fig. 5 shows the capacity of the FSO Markov channel for strong and weak turbulence where the parameter is the quasifrequency ν_0. Two values are chosen for the quasifrequency, $\nu_0 = 275$ Hz and $\nu_0 = 550$ Hz as in [11]. The values of α and β are the same as in Section III-C. $R_{s,550}$ and $R_{w,550}$ are the capacities for strong and weak turbulence when $\nu_0 = 550$ Hz, respectively. A similar notation is used when $\nu_0 = 275$ Hz. In Fig. 5, a number within parenthesis denotes the number of states of a corresponding Markov chain model. It can be noticed again that the capacity for the weak turbulence is larger than the capacity for the strong turbulence. The smaller the quasifrequency (corresponding to larger channel memory) the larger the capacity; however the difference in the capacity when the quasifrequency is doubled for the same turbulence regime is negligible. This is in accordance with the capacity results for the RF wireless channels that exhibit little difference for the similar change in the Doppler spread [10]. Also, for a fixed ν_0 and fixed turbulence regime, the difference between capacity curves decreases as the number of states of the Markov chain increases. Consequently, it can be conjectured that as the number of the Markov chain states increases, the capacity sequence will converge to a true value of the capacity since the resolution (or accuracy) of the Markov model increases. From plots, it can be concluded that 8-state Markov chain model gives a pretty good estimation of the FSO channel capacity.

In the simulations, the transition probabilities are computed by the following approach found in [10]. 1) It is assumed that the Markov states are equiprobable. 2) The fading levels I_k, $k = 0, \ldots, K$ are found by using distribution $p(i)$ having in mind equiprobability of states. 3) Once the fading levels are known, the crossover probabilities $p_{e,k}$ and the transition probabilities $p_{i,j}$ are computed by using (21) and (16)–(19), respectively. It is assumed that the channel symbol interval is $T_s = 10^{-5}$ s, which is much smaller than the reciprocal value of the quasifrequency, such that the FSO channel is slow-fading channel.

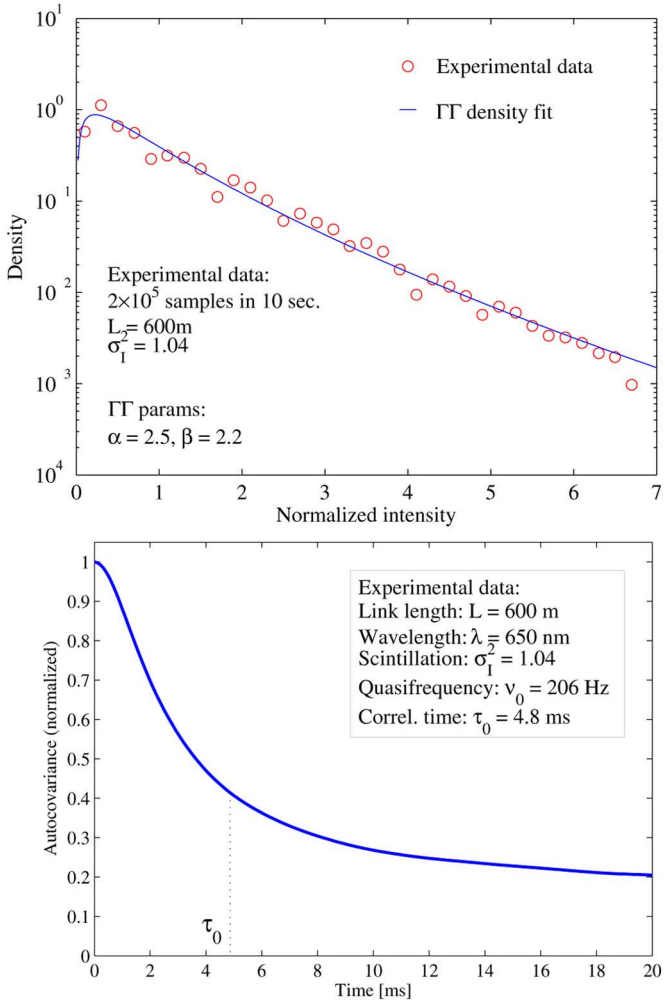

Fig. 6. (a) PDF of an experimentally recorded channel waveform with $\sigma_I^2 = 1.04$ (strong fluctuations). A gamma-gamma density is fitted to the experimental data to show the suitability of the model. (b) Normalized autocovariance of the channel waveform used in (a). The correlation time is $\tau_0 = 4.8$ ms and the quasifrequency is $\nu_0 = 206$ Hz.

D. Computation of the Channel Capacity From Experimental Data

We further evaluate the Markovian model using experimentally recorded FSO channel samples. These channel samples were obtained by means of an experimental apparatus similar to the setup shown in Fig. 1. It consists of a continuous-wave laser beam with wavelength 650 nm, which is expanded and projected toward a reflector 300 m away on a horizontal path. The reflected beam is collected by a telescope located next to the transmitter, thus completing a 600-m optical path. The collected light is focused on a multimode fiber whose other end is connected to an optical detector. The optical detector delivers a current proportional to the incoming optical signal that is recorded with an oscilloscope. The recorded waveforms deliver temporally correlated channel samples (that is, i_t in (1)), providing the most realistic way to evaluate the FSO channel.

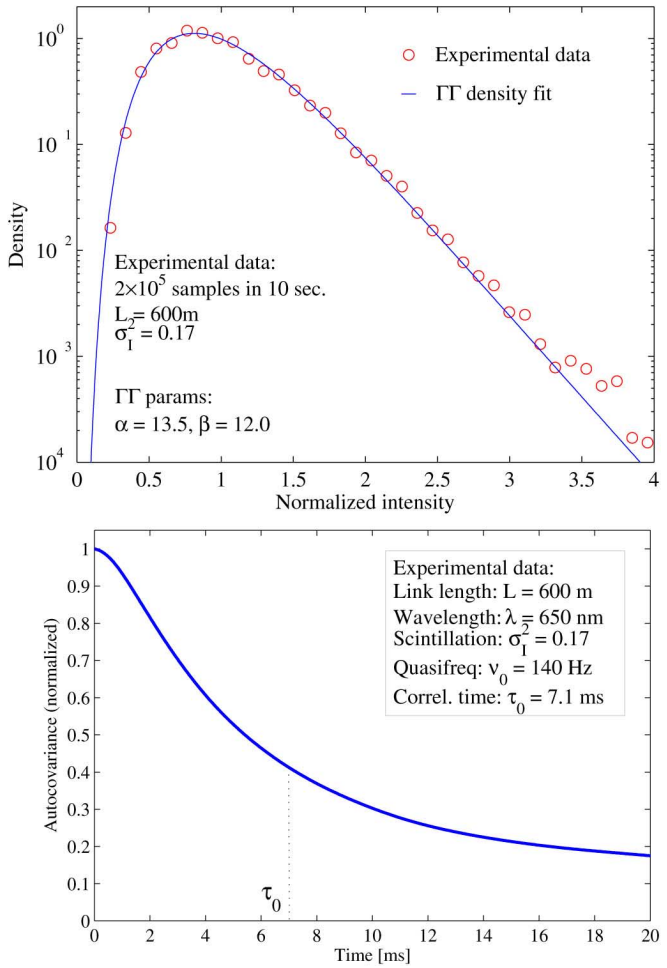

Fig. 7. (a) PDF of experimentally recorded channel samples with $\sigma_I^2 = 0.17$ (weak fluctuations). A gamma-gamma density is fitted to the experimental data to show the suitability of the model. (b) Normalized autocovariance of the channel waveform used in (a). The correlation time is $\tau_0 = 7.1$ ms and the quasifrequency is $\nu_0 = 140$ Hz.

Two channel waveforms are selected for this evaluation. The first waveform features a scintillation index $\sigma_I^2 = 1.04$, in the strong turbulence regime. Fig. 6(a) shows a histogram of the experimental channel samples. A gamma-gamma distribution has been fitted to these experimental data (with parameters $\alpha = 2.5$ and $\beta = 2.2$) to show the suitability of this analytical model. The autocovariance of the channel waveform, normalized to a maximum of one, is shown in Fig. 6(b). From this plot we compute the quasifrequency $\nu_0 = 206$ Hz using the Rice formula (20). The correlation time of the channel τ_0, which we define as the reciprocal value of the quasifrequency ν_0, is equal to 4.8 ms. In Fig. 7(a) we present the histogram of a channel waveform in the weak turbulence regime, with a scintillation index $\sigma_I^2 = 0.17$. In this case, the gamma-gamma density is fitted with $\alpha = 13.5$ and $\beta = 12.0$. As before, the normalized autocovariance of the channel waveform is computed, giving $\nu_0 = 140$ Hz and $\tau_0 = 7.1$ ms. This is shown in Fig. 7(b).

We have chosen a transmission rate of $R = 1$ Mbits/s, which corresponds to a channel symbol interval of $T_s = 10^{-6}$ s. The capacity is determined using a Markov model with 8 states for both experimental cases described above. Fig. 8 shows the

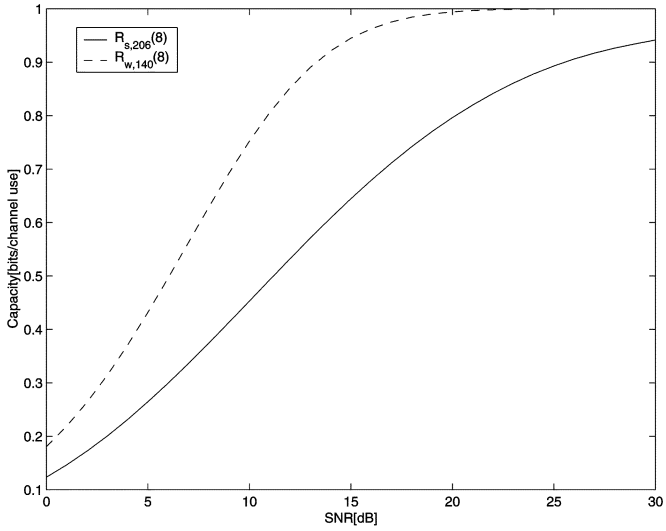

Fig. 8. Capacity versus SNR for the OOK transmission for a strong and weak turbulence, when the channel models are obtained from experimental data.

channel capacities for two studied scenarios, labeled $R_{s,206}$ in the strong turbulence case and $R_{w,140}$ in the weak turbulence case. The capacity curve in the latter case $(R_{w,140})$ reaches the maximum value of 1 bits/channel use at approximately 24 dB, while for the former case $(R_{s,206})$ even 30 dB is not sufficient to reach its saturation point.

From further extensive experiments and measurements, we have determined that a practical range for the quasifrequency ν_0 is between 100 Hz and 500 Hz.

V. Conclusions

The achievable rates and capacities of FSO communication channels are considered, subject to different assumptions on the turbulent channel memory and the CSI. For IID channels experiencing strong turbulence, it is shown that the CSI at the transmitter can be beneficial for low to moderate SNRs. Also, for strong turbulence conditions, the "positive" Gaussian input is comparable to $M = 2$ PAM, but it is inferior to $M \geq 4$ PAM. For weak turbulence regimes, the channel inversion may be more appropriate. When the CSI is absent, and the channel is modeled by a Markov process, the change of the capacity is insignificant as the quasifrequency varies.

References

[1] G. Caire and S. Shamai, "On the capacity of some channels with channel state information," *IEEE Trans. Inf. Theory*, vol. 45, no. 6, pp. 2007–2019, Sep. 1999.

[2] J. A. Anguita, I. B. Djordjevic, M. A. Neifeld, and B. V. Vasic, "Shannon capacities and error-correction codes for optical atmospheric turbulent channels," *J. Opt. Netw.*, vol. 4, no. 9, pp. 586–601, Sep. 2005.

[3] M. A. Al-Habash and R. L. Phillips, "Mathematical model for the irradiance probability density function of a laser beam propagating through turbulent media," *Opt. Eng.*, vol. 40, no. 8, pp. 1554–1562, Aug. 2001.

[4] E. Biglieri, J. Proakis, and S. Shamai, "Fading channels: Information-Theoretic and communications aspects," *IEEE Trans. Inf. Theory*, vol. 44, no. 6, pp. 2619–2692, Oct. 1998.

[5] T. H. Chan, S. Hranilovic, and F. R. Kschischang, "Capacity-achieving probability measure for conditionally Gaussian channels with bounded inputs," *IEEE Trans. Inf. Theory*, vol. 51, no. 6, pp. 2073–2088, Jun. 2005.

[6] A. J. Goldsmith and P. P. Varaiya, "Capacity of fading channels with channel side information," *IEEE Trans. Inf. Theory*, vol. 43, no. 6, pp. 1986–1992, Nov. 1997.
[7] A. Farid and S. Hranilovic, "Upper and lower bounds on the capacity of wireless optical intensity channels," in *Proc. ISIT 2007*, Nice, France, 2007.
[8] S. Hranilovic and F. R. Kschischang, "Capacity bounds for power- and band-limited optical intensity channels corrupted by Gaussian noise," *IEEE Trans. Inf. Theory*, vol. 50, no. 5, pp. 784–795, May 2004.
[9] M. Mushkin and I. Bar-David, "Capacity and coding for the Gilbert-Elliot channels," *IEEE Trans. Inf. Theory*, vol. 35, no. 6, pp. 1277–1290, Nov. 1989.
[10] H. S. Wang and N. Moayeri, "Modeling, capacity and joint source/channel coding for rayleigh fading channels," in *Proc. 1993 43rd IEEE Veh. Technol. Conf.*, May 1993, pp. 473–479.
[11] L. C. Andrews and R. L. Phillips, *Laser Beam Propagation Through Random Media*. Bellingham, WA: SPIE Press, 2005.
[12] J. Li Tiffany and M. Uysal, "Optical wireless communications: System model, capacity and coding," in *Proc. 2003 58th IEEE Veh. Technol. Conf.*, Oct. 2003, vol. 1, pp. 168–172.
[13] M. Uysal, S. M. Navidpour, and J. Li Tiffany, "Error rate performance of coded free-space optical links over strong turbulence channels," *IEEE Commun. Lett.*, vol. 8, pp. 635–637, Oct. 2004.
[14] M. Uysal, J. Li Tiffany, and M. Yu, "Error rate performance analysis of coded free-space optical links over gamma-gamma atmospheric turbulence channels," *IEEE Trans. Wireless Commun.*, vol. 5, no. 6, pp. 1229–1233, Jun. 2006.
[15] X. Zhu and J. M. Kahn, "Free-space optical communication through atmospheric turbulence channels," *IEEE Trans. Commun.*, vol. 50, pp. 1293–1300, Aug. 2002.
[16] S. O. Rice, "The mathematical analysis of random noise," *Bell Sys. Tech. J.*, vol. 23, pp. 282–332, 1944.

Stojan Z. Denic (S'04–M'06) received the B.Sc. and M.Sc. degrees in electrical engineering from the Faculty of Electronic Engineering, University of Nis, Serbia, in 1994 and 2001, respectively, and the Ph.D. degree from the School of Information Technology and Engineering, University of Ottawa, ON, Canada.

From 1996 to 2000, he was with the Telecom Serbia. He was a Research Assistant Professor with the Electrical and Computer Engineering Department, University of Arizona, Tucson until 2008. He is now with Toshiba Telecommunications Research Laboratory in Bristol, U.K. His research interests include information theory, communication over uncertain channels, control over communication channels, optical communications, and coding for wireless and digital recording channels.

Ivan Djordjevic (M'04) received the B.Sc., M.Sc., and Ph.D. degrees in electrical engineering from the University of Nis, Serbia, in 1994, 1997, and 1999, respectively.

Currently, he is an Assistant Professor of electrical and computer engineering at the University of Arizona, Tucson. He presently directs the Optical Communications Systems Laboratory (OCSL) within the ECE Department at the University of Arizona. He was with the University of the West of England, Bristol, U.K.; University of Bristol, U.K.; Tyco Telecommunications, Eatontown, NJ; and National Technical University of Athens, Greece. His current research interests include optical networks, error control coding, constrained coding, coded modulation, turbo equalization, OFDM, and quantum communications.

Dr. Djordjevic serves as an Associate Editor for *Research Letters in Optics* and *International Journal of Optics*. He is an author of more than 90 journal publications and over 70 conference papers.

Jaime Anguita (S'02–M'07) received the B.S. degree from Universidad Catolica, Santiago, Chile, in 1994 and the M.S. and Ph.D. degrees from the University of Arizona, Tucson, in 2004 and 2007, respectively, all in electrical engineering.

He worked for the European Southern Observatory and for a Chilean power distribution company. His research interests are optical communications, both free-space and fiber-based, channel characterization, modulation and error-control coding, and signal processing.

Dr. Anguita is a member of the Optical Society of America (OSA) and International Society for Optical Engineering (SPIE).

Bane Vasic (S'92–M'93–SM'02) received the B.Sc., M.Sc., and Ph.D. degrees in electrical engineering from the University of Nis, Serbia, in 1989, 1991, and 1994, respectively.

Currently, he is a Professor of electrical and computer engineering and mathematics at the University of Arizona, Tucson. Prior to this appointment, he was at Bell Laboratories in Allentown, PA. He authored a number of journal and conference articles and book chapters, and edited two books. His patents are implemented in Bell Lab chips. His research interests include coding theory, communication theory, constrained systems, and digital communications and recording.

Dr. Vasic is a Member of the Editorial Board of the IEEE TRANSACTIONS ON MAGNETICS, and was a Chair or Technical Program Chair for several workshops and conferences including 2003 and 2007 IEEE Communication Theory Workshop (CTW); 2004 DIMACS Workgroup and Workshop on Theoretical Advances in Information Recording; 2004 LANLWorkshop on Applications of Statistical Physics to Coding Theory; and 2006 Communication Theory Symposium within ICC.

Mark A. Neifeld (S'84–M'91) received the B.S.E.E. degree from the Georgia Institute of Technology, Atlanta, in 1985 and the M.S. and Ph.D. degrees in electrical engineering from the California Institute of Technology, Pasadena, in 1987 and 1991, respectively.

During the 1985-1986 academic year, he was also a Member of Technical Staff in the TRW Systems Engineering and Analysis Laboratory, Redondo Beach, CA. For one year, he held a postdoctoral position at the NASA Jet Propulsion Laboratories, Pasadena, where he studied the application of parallel image processing techniques to problems in target recognition. In August 1991, he joined the faculty of the Department of Electrical and Computer Engineering, University of Arizona, Tucson. He is also a member of the faculty of the Optical Sciences Center at the University of Arizona and has coauthored more than 50 conference and journal papers in the areas of optical storage, parallel coding and signal processing, optoelectronic device simulation and CAD, computer generated holography, character recognition, neural networks, and optical processing systems. His thesis work focused on the use of parallel access optical memories for image pattern recognition. He presently directs the Optical Computing and Processing Laboratory within the ECE Department at the University of Arizona.

Dr. Neifeld is a member of SPIE and APS. He has served on the organizing committees of numerous conferences and symposia. He has also been a two-term topical editor for *Applied Optics* and a three-time guest editor of special issues of *Applied Optics*.